

ANISOTROPY CHARACTERIZATION OF NON STATIONARY GREY LEVEL TEXTURES

Gérald Lemineur¹, Rachid Harba¹, Rachid Jennane¹

¹Laboratory of Electronics, Signals, Images

Polytech'Orléans, BP 6744, 45067 Orleans, France

phone: +33 (0)2 38 41 72 29, fax: +33 (0)2 38 41 72 45, email: rachid.harba@univ-orleans.fr

ABSTRACT

This communication deals with anisotropy characterization of grey level textures in a non stationary context. Three classes of characterization methods are tested. The first class of methods directly uses the non stationary data. We chose here the non stationary fractional Brownian motion (fBm) to model such images. The second class is based on a stationary approach. Thus, the image is to be stationarized first. The third class of methods is founded on stationary techniques too, but in a binary framework. For this reason, the original image must be stationarized and binarized first. All the proposed methods are tested on various grey level non stationary textures. Results show that all the techniques are in good agreement with the anisotropy visible on the data. The fBm based method is the only one that does not require any choice or adjustment of parameters. For a real application where the anisotropy really matters, this technique should be tested.

1. INTRODUCTION

Texture is an important feature in image analysis and understanding. An anisotropic texture shows different characteristics as the angle of analysis varies. It is the case for instance in material science [1] in which considerable literature on the subject can be found. Some texture can also be non stationary. It is seen in material science too [2] or in medical analysis [3] to give just two examples among the most well documented. Some works have been done to characterize anisotropic textures [4]. Identically, the non stationary case for grey level images has also been studied [5]. But, the anisotropic analysis of grey level images in a non stationary context is still an open problem. It is the purpose of this communication to compare various methods to assess anisotropy in such a background.

To take into account the non stationarity of grey level images, at least three kinds of techniques can be thought of.

The first class of methods directly uses the non stationary data. Among all the possible approaches, the non stationary fractional Brownian motion (fBm) of H parameter in]0,1[could model such images [6]. The key point is that H translates the roughness of a texture: the more H is close to 0, the more an image appears to be rough and the more H is close to 1, the more images are smooth [7]. In the case of anisotropic data, this fractal technique should be adapted

[8][9]. The proposed method was named Directional Averages Method (DAM) and will be tested in this work.

As non stationary data are in general difficult to analyze, a possible solution is to stationarized them first. In such a context, the most well known techniques are based on second order statistics. These methods take advantage of Co-Occurrence Matrices (COM) or Run Length Matrices (RLM). They will be included in this study.

The third class of methods uses stationary techniques too, but in a binary context. The original image is to be stationarized and binarized first. These well known methods are the Mean Intercept Length (MIL), the Star Length Distribution (SLD), and the Line Fraction Deviation (LFD). They will be incorporated in this work.

All these 6 methods need to be implemented for various directions to take anisotropy into account. To do so, and to avoid problems linked to the extraction of 1D lines in 2D images, only multiple angles of 45° are used. Thus, 8 directions are of interest. Results are represented on a polar diagram. A Fourier analysis of this polar diagram leads to a single anisotropy index.

This communication is organized as follows. First, we will explain in details the DAM since it is the most recent one. The other methods will be very briefly described. Then, they will be evaluated on various grey level non stationary textures.

2. FIRST CLASS OF METHODS

The first class of methods, and the most natural one, directly uses the non stationary data. The non stationary fractional Brownian motion (fBm) of H parameter in]0,1[could be a good model. The H parameter translates the roughness of the texture. To present the method, let us recall the spectral definition of a 2D isotropic fBm of H index and with variable $\mathbf{t}=(t_1,t_2)$ [10]:

$$B_H(\mathbf{t}) = \int_{\mathbb{R}^2} \frac{e^{i\mathbf{t}\cdot\xi} - 1}{|\xi|^{H+1}} dB^2(\xi), \quad (1)$$

where $B^2 = \{B^2(\xi) ; \xi \in \mathbb{R}^2\}$ is the 2D complex Brownian field depending on the frequency $\xi=(\xi_1, \xi_2)$, $\mathbf{t}\cdot\xi$ is the scalar product of \mathbf{t} and ξ , and $|\xi|$ is the modulus of ξ . A possible modification to take anisotropy into account is to replace H

by a π -periodic function of the angle $\theta = \arctg(\xi_2/\xi_1)$ taking values in the interval $]0,1[$. Such an anisotropic fBm can be written:

$$B_{H,\theta}(\mathbf{t}) = \int_{\mathbb{R}^2} \frac{e^{it \cdot \xi} - 1}{|\xi|^{H(\theta)+1}} dB^2(\xi). \quad (2)$$

A natural evaluation of the anisotropy would consist in measuring the parameter H of parallel lines extracted from an image and in repeating this analysis for a finished number of directions. But, this natural evaluation fails [11]. A new method, called Directional Averages Method (DAM), allows a precise measure of the fractal anisotropy [8][9]. It consists in averaging the 2D image along parallel lines and to estimate the H parameter of this signal. This is explained more precisely in the following.

Averaging an anisotropic fBm along parallel lines of direction φ , within a square integral window ψ of average 1, results in a Gaussian process $\{Y_{H,\varphi}(s); s \in \mathbb{R}\}$ of spectral representation:

$$Y_{H,\varphi}(s) = \int_{-\infty}^{+\infty} (e^{is\xi} - 1) g_{H,\varphi}(\xi) dB^1(\xi), \quad (3)$$

where $B^1 = \{B^1(\xi); \xi \in \mathbb{R}\}$ is the 1D complex Brownian process. The spectral density $g_{H,\varphi}$ is given by:

$$\begin{aligned} (g_{H,\varphi}(\xi))^2 &= \frac{1}{|\xi|^{2H(\varphi+\pi/2)+2}} \times \\ &\int_{-\infty}^{+\infty} \frac{|\xi|^{2H(\varphi+\pi/2)-2H(\varphi+\arctg\frac{\xi}{u})} |\hat{\psi}(u)|^2}{(1+(\frac{u}{\xi})^2)^{H(\varphi+\arctg\frac{\xi}{u})+1}} du. \end{aligned} \quad (4)$$

$\hat{\psi}$ is the Fourier transform of ψ . Therefore the spectral density $g_{H,\varphi}$ is equivalent at high frequency to:

$$\frac{C_\psi}{|\xi|^{H(\varphi+\pi/2)+1}} \quad (5)$$

with the constant $C_\psi = \sqrt{\int_{-\infty}^{+\infty} |\hat{\psi}(u)|^2 du}$.

Let us recall that the spectral density of 1D fBm is equivalent to $1/|\xi|^{H+0.5}$. It clearly shows that the averaged process $Y_{H,\varphi}$ behaves at high frequency as a 1D fBm of index $H(\varphi+\pi/2)+0.5$. It is then possible to estimate $H(\theta)$ of the 2D image from the knowledge of the 1D averaged process. Thus, the roughness of an anisotropic non stationary grey level texture is clearly analyzed using the DAM.

To sum up, this method can be simply explained as follows:

- extract N parallel lines of an image in the direction θ ;
- average each line; a signal composed of N samples results;

- on the last signal, compute the H parameter using the variance method of Pentland which is very easy to implement [7];
- by subtracting 0.5 to the last value, the H parameter in the direction $\theta + \pi/2$ of the original data is obtained.

Finally, it should be noticed that DAM does not require any choice or adjustment of parameters.

3. SECOND CLASS OF METHODS

The second class of methods to characterize the anisotropy of non stationary textures is based on a grey level analysis of the image in a stationary context. Thus the image is first to be stationarized.

The most well known techniques that are based on this stationary approach are second order statistics, namely Co-Occurrence Matrices (COM) [12] and Run Length Matrices (RLM) [13].

The COM consists in constructing M , a $n \times n$ matrix, where n is the number of grey-levels within the image. For reasons of efficiency, the number of grey levels of the image is reduced to eight. The matrix $M(i,j,d,\theta)$ is defined as the number of pixel pairs having the intensities i and j , separated by a distance d for a direction θ . We can evaluate the energy which is defined as follows:

$$E(d,\theta) = \sum_i \sum_j M(i,j,d,\theta)^2. \quad (6)$$

In the framework of this study, this parameter gives the best results among all that can be extracted out of this method. In addition, we choose $d=3$.

For the RLM, a matrix $M(i,l,\theta)$ stores the number of grey level runs with grey level i , length l , in the θ direction. It is a $L \times n$ matrix where L is the maximum length of a run and n the maximum grey level value. As for the COM, the number of grey levels of the image is reduced to eight. Among the feature typically extracted from the run length matrix, we calculated the long run emphasis which gives the best results in our case. This parameter is estimated as follows:

$$LRE(\theta) = \sum_i \sum_l l^2 M(i,l,\theta). \quad (7)$$

4. THIRD CLASS OF METHODS

The third class of methods is based on a binary analysis of the image in a stationary context. Thus the image is first to be stationarized as previously. But, in addition, they also have to be binarized.

These well known methods are the Mean Intercept Length (MIL) [14], the Star Length Distribution (SLD) [15] and the Line Fraction Deviation (LFD) [16].

The MIL is defined as the mean length of the bright and dark line segments on an analyzed grid and allows to estimate the main orientation of the image texture. At first, the number of dark and bright intercept (N) along all the lines of the image in a direction θ is calculated. Finally, the MIL is equal to the total length of analysed lines L divided by the number of intercepts N :

$$MIL(\theta) = \frac{L}{N}. \quad (8)$$

For the SLD, a regularly spaced point grid is generated on the binarized image. Only points falling within the phase of interest are retained. A test line of direction θ is generated from each point and is stopped at the black and white interface. Then we summated the lengths of the lines for a direction θ to obtain $l(\theta)$. The following parameter results:

$$SLD(\theta) = \frac{\sum l^2(\theta)}{\sum l(\theta)} \quad (9)$$

To estimate the LFD index of an image in a direction θ , the fraction of bright pixels is estimated for each line following θ . The parameter $LFD(\theta)$ corresponds to the standard deviation of these fractions.

5. ANISOTROPY INDICATOR

All these 6 methods need to be implemented for various directions to take anisotropy into account. To do so, and to avoid problems linked to the extractions of 1D lines in 2D images, only multiple angles of 45° are used. Thus, 8 directions are of interest. A polar diagram results of these analyses. One of these polar diagrams is presented in figure 1 for the LFD method and for grass (small dashed line) and straw (large dashed line) which are presented in figure 2. It is obvious that straw is more anisotropic than grass.

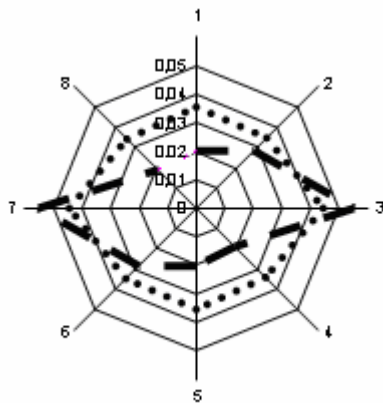


Figure 1: a polar diagram for grass (small dashed line) and straw (large dashed line) for the LFD method.

The polar diagram as presented in figure 1 brings information about the anisotropy. To extract this information, we model the polar diagram by an ellipse. We then calculate an anisotropic degree which is equal to the main axis divided by the small axis of the ellipse. For that purpose we use the Fourier decomposition. The discrete polar diagram D composed of N samples is considered as a 2π -periodic function and is decomposed into coefficients C_n :

$$C_n = \frac{1}{N} \sum_{k=0}^{N-1} D\left(\frac{2k\pi}{N}\right) e^{\frac{-i2\pi nk}{N}} \quad (10)$$

C_0 corresponds to the ray of the mean square circle. C_2 quantifies the elliptic character of the polar diagram. The main axis of the mean square ellipse is equal to $C_0 + \text{modulus}(C_2)$, and the small axis to $C_0 - \text{modulus}(C_2)$. We define the anisotropy degree AD by:

$$AD = \frac{C_0 + \text{modulus}(C_2)}{C_0 - \text{modulus}(C_2)} \quad (11)$$

AD is equal to 1 for isotropic images, and greater than 1 for anisotropic ones.

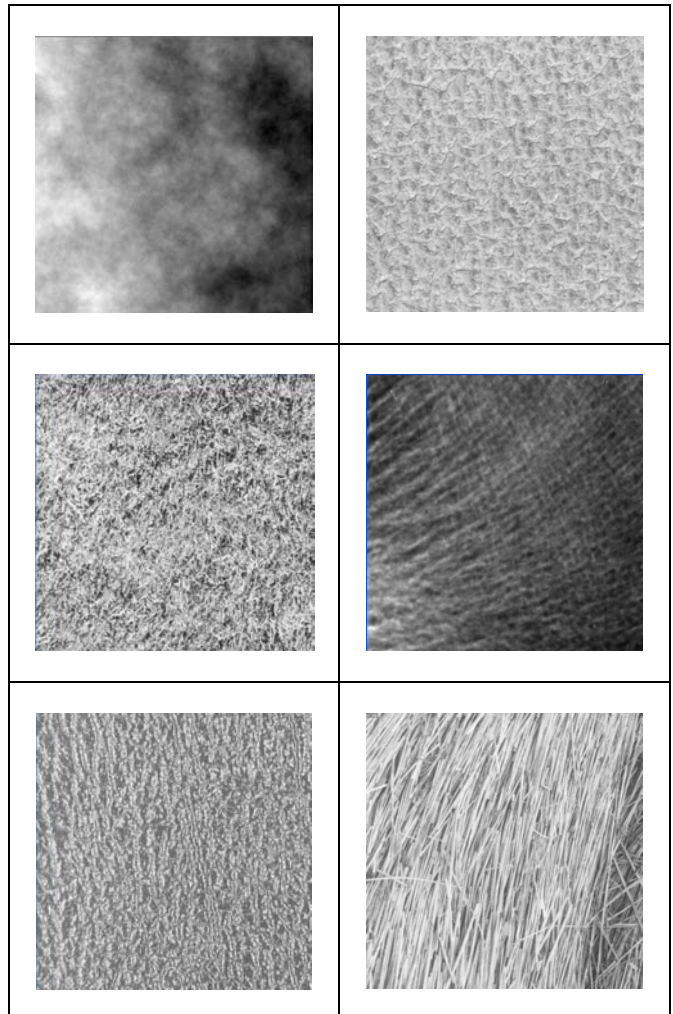


Figure 2: non stationary grey level textures that will be tested concerning their anisotropy. From left to right and top to bottom: a synthetic isotropic fBm image, pig skin, grass, calcaneum radiograph, pressed calf leather, and straw.

6. TESTED IMAGES AND PREPROCESSING

We will test the 6 non stationary grey level textured images presented in figure 2. The first one is a synthetic fBm image. It is expected that the methods give an AD equal to one. The five other are natural textures which clearly show anisotropy as well as first order non stationarity (the average grey level is not identical in all regions). Four images are extracted from the Brodatz data base (pig skin, grass, pressed calf leather and straw). The last one is a radiograph corresponding to the trabecular bone which is a porous material. It is organized so as to supply a mechanical resistance adapted to various constraints. Trabeculae in the directions undergoing the main forces are more numerous, bigger and thus deteriorate less quickly. These non uniform changes due to

riorate less quickly. These non uniform changes due to osteoporosis induce variations in the degree of anisotropy.

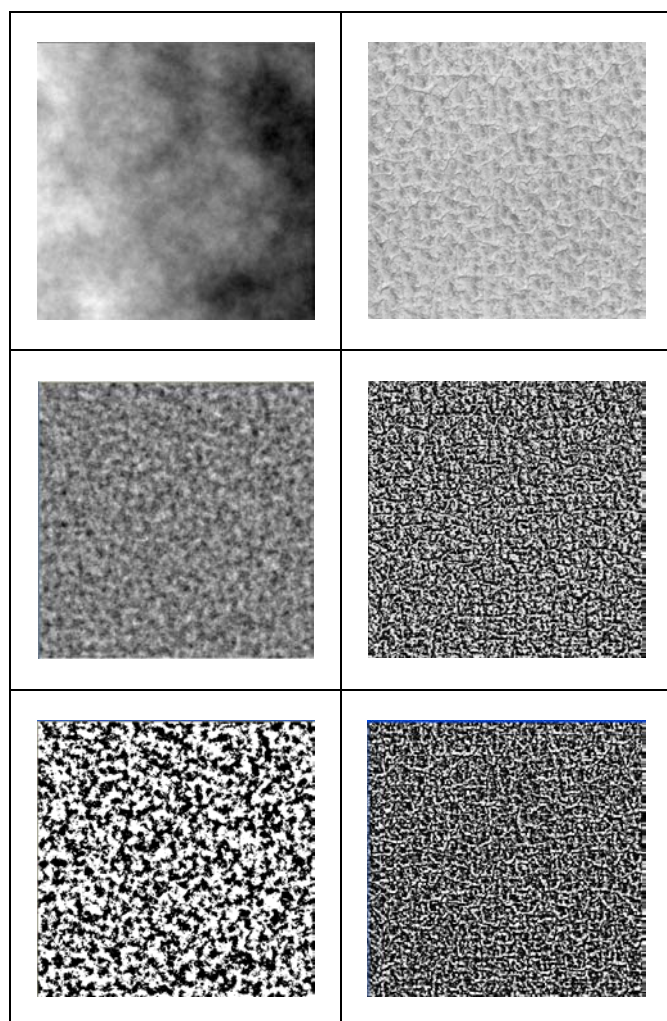


Figure 3: First row: isotropic fBm and pig skin images. Second row: stationarized images. Third row: stationarized and binarized images.

These images are directly used as entries for DAM.

For the COM and RLM, they are to be stationarized. A possible technique to render the image stationary is to remove the low frequency trends from the original image. They are calculated by a low pass filtering of the original image. The low pass filter is a square filter of size 25×25 with only one as coefficients

Finally, for MIL, SLD and LFD, images are also binarized. As the histograms are unimodal, thresholds are chosen as the maximum value of the smoothed histograms.

Related images are presented in figures 3, 4 and 5.

7. RESULTS

The 6 images are tested concerning their anisotropy using the 6 methods previously described. Results are presented in table 1.

For these images, AD is between 1 and 2 so that the variations can easily be interpreted.

Results show a good general agreement. First, on the synthetic isotropic fBm image, AD is always lower than 1.026 which is close to the theoretical value of 1 for perfect isotropic objects. Second, on straw which visually is the most anisotropic one, all the techniques have their maximal value. For other images where the anisotropy is mild, the results may be different relatively to the methods. Reasons for these differences could be a subject of a thorough experiment and is beyond the scope of this work. Only a practical application can decide which technique is the best for a given context. As a final remark, the processing cost for all methods is equivalent.

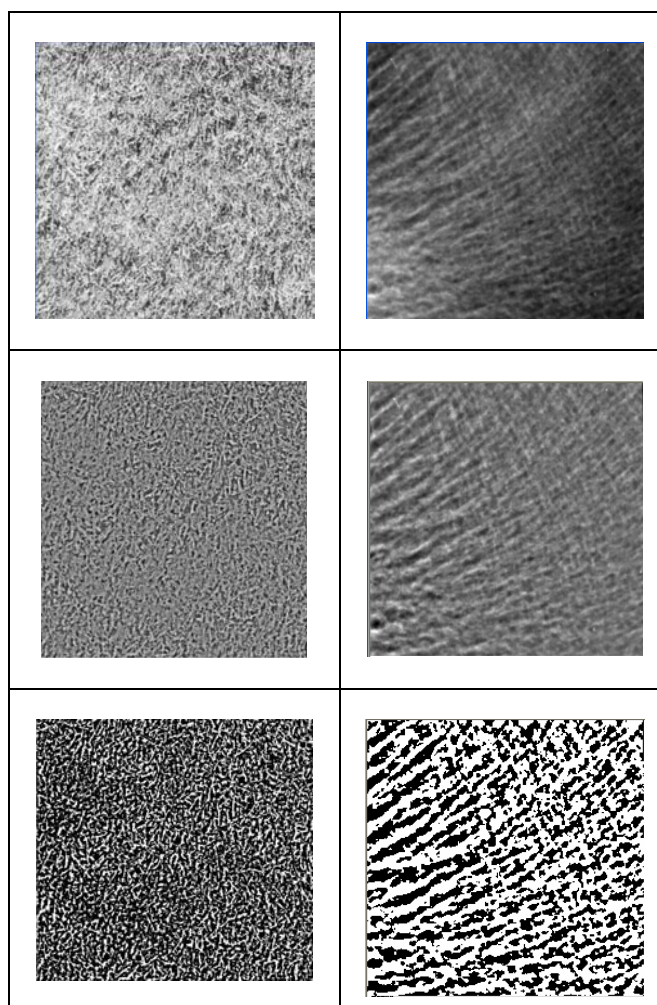


Figure 4: First row: grass and calcaneum images. Second row: stationarized images. Third row: stationarized and binarized images.

8. CONCLUSION

In this communication we have presented 6 methods for the analysis of anisotropy of grey level textures in a non stationary context. The first one (DAM) directly uses the non stationary data. Two of them (COM and RLM) are based on a stationary approach. The last three ones (MIL, SLD, and LFD) are founded on stationary techniques too, but in a binary perspective. All the proposed methods were tested on six grey level non stationary textures. Results show that all the methods are in good agreement with the anisotropy visible on the data. DAM is the only method that does not

need any choice or adjustment of parameters. For a real application where the anisotropy really matters, this method is a technique that should be tested

In a near future, we will test these methods to characterize the anisotropy of trabecular bone radiographs for an early diagnosis of osteoporosis.

	DAM	COM	RLM	MIL	SLD	LFD
Isotropic fBm	1.0097	1.0038	1.0053	1.0015	1.0135	1.0253
Pig skin	1.1500	1.0603	1.1033	1.0507	1.1636	1.1151
Grass	1.2830	1.0693	1.1167	1.0470	1.2482	1.1276
Calcaneum radiograph	1.1013	1.1477	1.2205	1.1245	1.4333	1.2431
Pressed calf leather	1.3666	1.1481	1.2182	1.0553	1.4395	1.3136
Straw	2.0756	1.5293	1.8418	1.3246	2.1781	1.8349

Table 1: Anisotropy Degree (AD) on the 6 tested images using the 6 techniques.

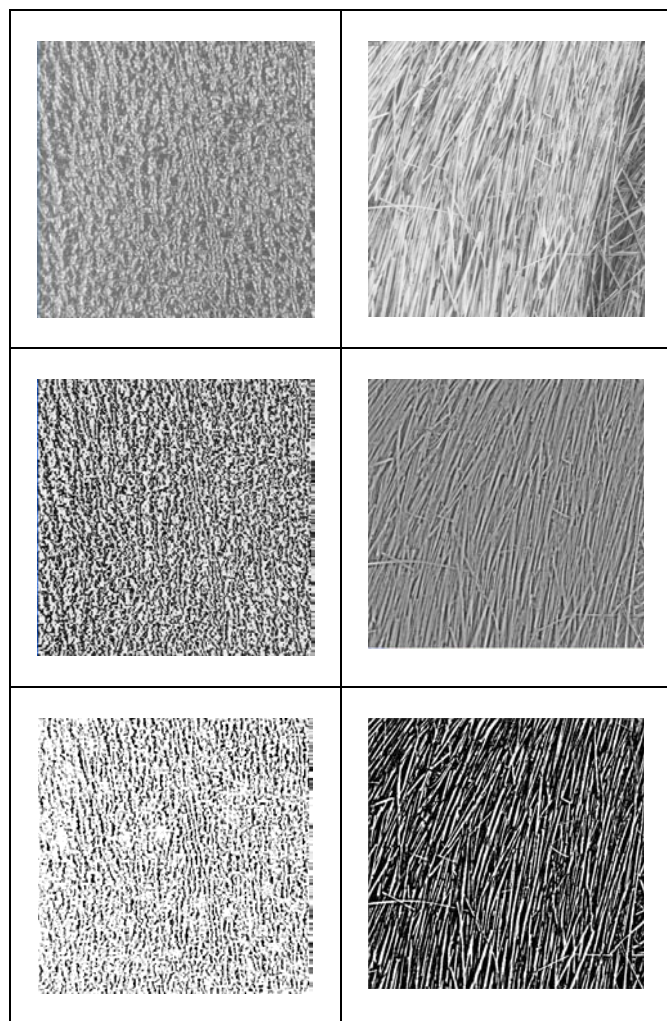


Figure 5: First row: pressed calf leather and grass images. Second row: stationarized images. Third row: stationarized and binarized images.

REFERENCES

[1] K. Helming, J. Probst, R. Thull, L. Weislak, "Preferred orientations in coated titanium implants", in *Proc. of the Int. Conf. on Texture and Anisotropy of Polycrystals*. pp. 667-672, 1998.
 [2] M Zabat, M. Veyer-Besancon, R. Harba, S. Bonnamy, H. Van Damme, "*Surface Topography and Mechanical Properties of Smectite Films*", *Progr. Colloid. Polym. Sci.*, Vol. 105, pp. 96-102, 1997.

[3] R. Harba, G. Jacquet, R. Jennane, T. Loussot, C. L. Benhamou, E. Lespessailles, D. Tourlière, "*Determination of Fractal Scales on Trabecular Bone X-Ray Images*", *Fractals*, Vol. 2, N° 3, pp. 451-456, 1994.
 [4] C. Germain, J.P. Da Costa, O. Lavialle, P. Baylou, "Multiscale estimation of vector field anisotropy. Application to texture characterization", *Signal Processing*, Vol 83, pp. 1487-1503, juillet 2003.
 [5] X. Descombes, M. Sigelle, F. Prêteux, "GMRF Parameter Estimation in a non-stationary Framework by a Renormalization Technique: Application to Remote Sensing Imaging" *IEEE Trans. Image Processing*, 8(4): pp. 490-503, 1999.
 [6] B. B. Mandelbrot, J. W. Van Ness, "Fractional Brownian Motion, Fractional Noises and Applications," *SIAM*, Vol. 10, N° 4, pp. 422-438, 1968.
 [7] A. P. Pentland, "Fractal-Based Description of Naturel Scenes," *IEEE transactions on Pattern analysis and Machine Intelligence*, N° 6, pp. 661-674, 1984.
 [8] A. Bonami, A. Estrade, "Anisotropic Analysis of some Gaussian Models " *The Journal of Fourier Analysis and Applications*, Vol. 9, pp. 215-236, 2003.
 [9] G. Lemineur, R. Harba, R. Jennane, A. Estrade, L. Benhamou, "*Fractal anisotropy measurement of bone texture radiographs*," *IEEE ISCCSP 2004*, pp. 275-278, 2004.
 [10] S. Reed, P. C. Lee, T. K. Truong, "Spectral Representation of Fractional Brownian Motion in n Dimensions and its Properties," *IEEE Trans. on Inf. Theory*, Vol. 41, N° 5, pp. 1439-1451, 1995.
 [11] S. Davies, P. Hall, "Fractal Analysis of Surface Roughness by Using Spatial Data," *J. R. Stat. Soc.*, Vol. 61, Part 1, pp. 3-37, 1999.
 [12] R.M. Haralick, K. Shanmugam, I. Dinsten,"Textural Features for Image Classification", *IEEE Trans. on SMC*, vol. 3, n° 6, pp 610-621, 1973.
 [13] M.M. Galloway, "Texture Analysis Using Gray Level Run Length", *Computer Graphics and Image Processing*, 4, pp. 172-179, 1975.
 [14] J.E. Hilliard, "Specification and Measurement of Microstructural Anisotropy", *Trans Metallurg Soc AIME*, 224, pp. 1201-1211, 1962.
 [15] T.H. Smit, E. Schneider, A. Odgaard, "Star Length Distribution: A Volume-Based Concept for Characterization of Structural Anisotropy", *Journal of Microscopy*, Vol.191, pp. 249-257, 1998.
 [16] W.G.M. Geraets, "Comparison of Two Methods for Measuring Orientation", *Bone*, Vol. 23, N° 4, pp. 383-388, October 1998.